Biomaterials Science

Enhanced tumor-targeted gene delivery by bioreducible polyethylenimine tethering EGFR divalent ligands

Journal:	*Biomaterials Science*
Manuscript ID:	BM-ART-01-2015-000004.R1
Article Type:	Paper
Date Submitted by the Author:	31-Jan-2015
Complete List of Authors:	Lee, Duhwan; POSTECH, Chemistry Lee, Yeong Mi; POSTECH, Chemistry Kim, Jihoon; POSTECH, Chemistry Lee, Myung Gyu; Korea Research Institute of Biosciences and Biotechnology (KRIBB), Kim, Won Jong; Pohang University of Science and Technology, Chemistry

Enhanced tumor-targeted gene delivery by bioreducible polyethylenimine tethering EGFR divalent ligands.

Duhwan Lee[a,†], Yeong Mi Lee[a,†], Jihoon Kim[a], Myung Kyu Lee[b] and Won Jong Kim[a,*]

[a] *Center for Self-assembly and Complexity, Institute for Basic Science and Department of Chemistry, Pohang University of Science and Technology (POSTECH) 77 Cheongam-ro, Nam-gu, Pohang 790-784, Republic of Korea.*

[b] *Bionanotechnology Research Center, KRIBB, 125 Gwahak-ro, Yuseong-gu, Daejeon 305-806, Republic of Korea*

**Corresponding author. Tel: +82-54-279-2104; fax: +82-54-279-3399*

E-mail address: wjkim@postech.ac.kr

[†]*These authors contributed equally to this work.*

Abstract

This work demonstrates successful delivery of gene to the EGFR-overexpressed cancer cells by using a rationally designed branched GE11 peptide as a targeting ligand. In addition, we exploited the effect of the divalent structure of branched GE11 peptide on the gene delivery and tumor targeting efficiency, compared to monovalent GE11 peptide. The GE11 or branched GE11-tethered polymers were successfully synthesized, which are composed of a targeting peptide, disulfide crosslinked low molecular weight polyethylenimine and polyethylene glycol. Here, we evaluated the physicochemical properties, cytotoxicity and *in vitro* transfection efficiency and *in vivo* biodistribution of the GE11 or branched GE11 tethered polyplexes. Our results demonstrated that GE11 or bGE11-tethered gene delivery carriers showed efficient gene condensing ability, enhanced transfection efficiency and targeting ability with low cytotoxicity. Interestingly, branched GE11-tethered polymer showed the higher targeting ability to EGFR-overexpressed cancer cells *in vivo* than the GE11-tethered polymer. Therefore, this branched structure of targeting ligand has the potential for providing the novel strategy to design efficient targeted delivery system.

Introduction

For efficient polymeric delivery system, it is crucial to deliver precisely gene/polymer complex (polyplex) or drug into targeted tissue or organ. To solve this issue, researchers have developed numerous targeting ligands which can bind to the specific receptor overexpressed on the target tissues or organs.[1-3] Enhanced targeted delivery of payloads has been attained by using combination of ligands and receptors; folate/folate receptor, RGD peptide/integrin $\alpha_v\beta_5$, NGR peptide/aminopeptidase N receptor and epithermal growth factor (EGF)/EGF receptor (EGFR).[4-7] Among them, EGFR has been considered as one of the promising targets for gene and drug delivery system because of its overexpression in lung, liver, head, neck and a wide spectrum of human cancers from epithelial origin.[8-9] Researchers have shown enhanced targeting and delivery efficiency of therapeutic genes or drugs by tethering EGF to polymers, carbon nanotubes, liposomes, and dendrimers.[10-13] However, EGF itself is at risk for activating the EGFR, which leads cell proliferation and reduces antitumor effect of a therapeutic gene or drug.[14] As substitute for EGF, GE11 peptide (YHWYGYTPQNVI) was found by phase display library, which binds to the receptor as well as has low mitogenic activity.[15]

The structure of targeting ligands is important issue in developing the targeted delivery system.[16-18] For example, the cyclic form of NGR or RGD has shown better binding affinity to each receptor than linear form because restriction of structures enhances the receptor-ligand interactions by stabilizing the bent conformation of peptide.[19,20] In addition, the multivalent interactions between ligand and target molecules are widely utilized in biological process, such as the adhesion of a virus to the surface of a cell, binding of transcription factors to multiple sites on DNA, and recognition of antigens by antibodies.[21-24] These multivalent interactions are generally much stronger than monovalent interactions.[21] However,

the delivery system utilizing the multivalent form of targeting ligand has yet to be evaluated. Therefore, we used two types of targeting peptides which are structurally different. One is GE11 peptide itself, and the other is branched GE11 (bGE11) which has two ligands in one peptide.

Recently, we reported the efficient gene delivery system composed of bioreducible branched polyethylenimine (BPEI-SS), polyethylene glycol (PEG) and targeting peptide.[25-27] Branched polyethylenimine (BPEI), which is the representative cationic polymers for gene delivery, has the molecular weight (MW) dependency in transfection efficiency and cytotoxicity. It has been reported that BPEI with a high MW (> 25 kDa) shows high transfection efficiency and low biocompatibility, while BPEI with a low MW (< 1.8 kDa) shows low transfection efficiency and low cytotoxicity.[28] The shortcomings of BPEI can be overcome by introducing the disulfide linkage to the low MW BPEI. BPEI-SS shows the high transfection efficiency by forming stable polyplex with pDNA in the extracellular compartments. Subsequently, BPEI-SS are degraded by reductive conditions in intracellular compartments and shows the low cytotoxicity.[29] In addition, the conjugation of PEG moiety provides the stability in blood and biocompatibility of polyplex *in vitro* and *in vivo*.

In this study, we introduced two structurally different EGFR-targeting peptides to BPEI-SS-PEG and evaluated their physicochemical properties, *in vitro* transfection efficiency, cytotoxicity, cellular uptake efficiency and *in vivo* targeting efficiency (Figure 1).

Experiment

Materials

BPEI with MW 25,000 Da (BPEI25k), propylene sulfide, 3-(4,5-dimethylthiazol-2-yl)-2,5-diphenyltetra-zolium bromide (MTT) were purchased from Sigma-Aldrich (St. Louis, MO, USA). BPEI with MW 1,200 Da (BPEI1.2k) was obtained from Polyscience, Inc. (Warrington, PA, USA). Methanol, diethyl ether and dimethyl sulfoxide (DMSO) were purchased from Samchun pure chemical (Pyeongtaek, Korea). A dialysis membrane with molecular weight cut-off (MWCO) of 10 kDa was purchased from Spectrum Laboratories (Rancho Domingues, CA, USA). YOYO-1 iodide was obtained from Invitrogen (Eugene, OR, USA). Mounting medium for fluorescence with DAPI was purchased from VECTOR (Berlingame, CA, USA) and Cy5.5 NHS ester was obtained from GE healthcare (Little Chalfront, UK). Heterobifunctional polyethylene glycol with MW 5,000 Da (α-maleimide-PEG-ω-*N*-hydroxysuccinimide ester polyethylene glycol, MAL-PEG-NHS) was purchased from NOF Corporation (White Plains, NY, USA). GE11 peptide and branched GE11 (bGE11) peptide were prepared by solid phase peptide synthesis (GE11 = YHWYGYTPQNVIGRC and bGE11 = $(YHWYGYTPQNVI\text{-}GG)_2$-KGRC). Agarose powder and Tris-acetate-EDTA (TEA) buffer were purchased from bioneer Corp. (Daejeon, Korea). Dulbecco Modified Eagle's medium (DMEM) and Roswell Park Memorial Institute medium (RPMI 1640), penicillin-streptomycin, fetal bovine serum (FBS) and Dulbecco's phosphate buffered saline (DPBS) were obtained from Corning (Manassas, VA, USA). A luciferase assay system with reporter lysis buffer was purchased from Promega (Madison, WI, USA), Bradford protein assay reagent was purchased from Pierce Chemical Co. (Rockford, IL, USA). A549, HuH-7 and NIH3T3 cell lines were obtained from the Seoul National University Cell Bank (Seoul, Korea).

Purification of pDNA

Plasmid DNA (pDNA) encoding luciferease were propagated in a chemically competent DH5α strain (GibcoBRL, Rockville, MD, USA) and prepared with a GeneJET Plasmid Maxiprep Kit (Thermo scientific, Waltham, MA, USA). The concentration of pDNA was determined by measuring absorbance at 260 nm, and we found optical density at 260 to 280 nm in the range 1.8-1.9.

Synthesis of bioreducible branched polyethylenimine (BPEI-SS)

BPEI-SS was synthesized by previously reported methods with some modification.[29] Briefly, BPEI1.2k (1 g) in 20 mL vials was dissolved in 10 mL deionized water (DW) and pH of the solution was adjusted to 7.2 by adding 1 M HCl. The solution was lyophilized for 2 days. The resultant solid was dissolved in methanol and the solution was purged with nitrogen for 15 min. Propylene sulfide (7 eq.) was added by a syringe, then the reaction mixture was stirred at 60 ^{o}C for 24 h. The product was purified by precipitation in cold diethyl ether twice, and the degree of thiolation was measured using ^{1}H NMR in D_2O (Bruker 300 MHz). To synthesize BPEI-SS, BPEI-SH was dissolved in DMSO and oxidative crosslinking was performed by stirring the solution at room temperature for 48 h. Finally, the product was obtained by dialysis (MWCO 10 kDa) against DW and following lyophilization.

Synthesis of peptide-tethered bioreducible BPEI (BPEI-SS-PEG-GE11 or BPEI-SS-PEG-bGE11)

MAL-PEG-NHS (1 eq.) and GE11 or bGE11 peptides (1.2 eq. to maleimide groups) were dissolved in anhydrous DMSO and stirred at room temperature for 4 h. Next, BPEI-SS (19 eq. to NHS group) dissolved in DMSO was added to the solution. The reaction mixture was stirred at room temperature for 48 h. Finally, the product was obtained by dialysis (MWCO

10 kDa) against DW and following lyophilization. The chemical structure of BPEI-SS-PEG-GE11 (or bGE11) was analyzed by ^{1}H NMR in D_2O. Conjugation ratio of peptide to polymer was determined by fluorescence spectrometry (Shimadzu, Japan). Free peptide was used to draw a calibration curve for fluorescence intensity at known concentration. As a control, PEG-conjugated BPEI-SS (BPEI-SS-PEG) without targeting peptide was synthesized by using para-nitrophenylchloroformate (pNPC)-activated methoxy PEG.

Preparation of polyplex

Polyplexes (polymer/pDNA complex) with $1 \leq N/P \leq 15$, (where N is the molar amount of nitrogen in the polycation and P is the molar amount of phosphate in the pDNA) were prepared by adding polymer solution to the pDNA solution in PBS buffer. The polyplexes were incubated at room temperature for 30 min.

Agarose gel retardation assay

Polyplexes with various N/P ratios were loaded onto 1 % (w/v) agarose gel containing ethidium bromide (EtBr, 0.5 μg/mL) with a 6x loading dye. Electrophoresis was conducted at a constant voltage of 100 V for 20 min in 0.5x TAE buffer (Tris-acetate-EDTA). Naked pDNA (200 ng in 10 μL) was used as a control. The gel was analyzed on a UV illuminator to observe the position of the complexed pDNA relative to that of the naked pDNA.

Size and zeta potential measurements

Polyplexes were prepared at various N/P ratios and diluted using PBS buffer (pH 7.4, 140 mM NaCl). The final pDNA concentration was adjusted to 3 μg/mL. The particle size and zeta potential of each polyplex were measured by using a Zetasizer Nano S90 and Z (Malvern Instruments, Malvern, U.K.), respectively.

Cell Culture

EGFR overexpressed (EGFR-positive) adenocarcinomic human alveolar basal epithelial cell line (A549) and human hepato cellular carcinoma cell line (Huh-7) were cultured in RPMI164 medium and EGFR-negative mouse embryo fibroblast (NIH3T3) cell line were cultured in DMEM medium. Both medium contains 10 % FBS and 1% antibiotics and cells were grown and maintained in a humidified atmosphere with 5 % CO_2 at 37 ^oC.

MTT assay

The cytotoxicity of polyplexes was evaluated by the standard MTT assay protocol. Briefly, cells were seeded onto 96-well plates at a density of 5×10^3 cells/well and incubated for 24 h. pDNA (0.1 μg/μL) was complexed with the polymer at predetermined N/P ratios in PBS. Cells were incubated with polyplex in 100 μL of serum free media for 4 h, then incubated for 20 h in 200 μL of fresh media containing 10 % FBS. Next, media were replaced with 200 μL of fresh media and 20 μL of 5 mg/mL MTT solution were added. After 4 h, the media was removed and 200 μL of DMSO was added to each well to dissolve the internalized purple formazan crystals. An aliquot of 100 μL was taken from each well and transferred to a fresh 96-well plate. The absorption was measured at 570 nm using a microplate spectrofluorometer (VICTOR3 V Multilabel Counter, Perkin-Elmer-Wellesley, MA, USA). The control cells which were not exposed to the transfection system, were used to represent 100 % cell viability. The results are presented as mean and standard deviation (n = 3).

Luciferase reporter gene assay

Cells were seeded on 24-well plates at an initial density of 6×10^4 cells/well and were incubated for 24 h in 500 μL of media containing 10 % FBS at 37 ^oC in a humidified atmosphere with 5 % CO_2. pDNA (0.1 μg/μL) was complexed with the polymer at

predetermined N/P ratios in PBS. Cells were incubated with the polyplex in 250 μL of serum-free media for 4 h, then incubated for 20 h in 500 μL of media containing 10 % FBS. The cells were washed twice with 500 μL of PBS and lysed by adding 200 μL of lysis buffer. Luciferase gene expression was measured by using a microplate spcetrofluorometer and luciferase assay system. The results are presented as mean and standard deviation (n = 3).

Flow cytometry

Cells were seeded in 12-well plates at a density of 1×10^5 cells/well and incubated for 24 h. pDNA was labeled with YOYO-1 iodide for 12 h before use. YOYO-labeled pDNA (0.1 μg/μL) was complexed with polymer at N/P ratio of 10 in PBS buffer and incubated for 30 min. Cells were incubated with polyplex for 4 h in serum-free media. After incubation, cells were washed twice with PBS and then trypsinized. The harvested cells were centrifuged and supernatant was removed, then the cells were fixed with 4 % paraformaldehyde solution at 4 °C overnight. Paraformaldehyde solution was removed by centrifugation, then the cells were resuspended in PBS. The cells were analyzed using a FACS Caliber (Becton Dickinson, San Jose, CA, USA) and Becton Dickinson Cell Quest Software following the manufacturers' protocol.

***In vivo* imaging**

The POSTECH Biotech Center Ethics Committee approved all of the animal experiments in this study. *In vivo* near-infrared (NIR) imaging was performed using an IVIS spectrum small-animal *in vivo* imaging system (Caliper Life Science) located at the Pohang Center of Evaluation of Biomaterials (Pohang Technopark). We evaluated the fluorescence intensity of the polyplexes labeled with Cy5.5 at an N/P ratio 10 by using Cy5.5 (ex = 675 nm, em = 740 nm) filter set. To investigate the targeting efficiency of GE11- or bGE11-conjugated and non-

conjugated polyplexes, A549 cells were inoculated subcutaneously into the right flank of female BALB/c-nu/nu mice. After 4 weeks, the Cy5.5 labeled polyplexes (N/P = 20, 10 μg of pDNA) were injected in mice via a tail vein. Mice were anesthetized with 2 - 3 % isoflurane and placed into the IVIS Spectrum system. Images were taken 4 h after injection. After 24 h from injection, A549 xenografted mice were sacrificed for *ex vivo* imaging, and their major organs were collected. Each organ was rinsed with PBS three times, mounted on a board, and fluorescence images were taken by IVIS Spectrum system.

Results and discussion

Synthesis and characterization of bioreducible polymers with targeting ligands

Prior to synthesize the bioreducible BPEI with targeting ligands, we firstly synthesized thiolated BPEI (BPEI-SH) by using propylene sulfide as a thiolation agent at 7 equiv. to low MW BPEI1.2k (Figure S1). Thiolation of BPEI was conducted by the ring opening reaction between propylene sulfide and primary amine or secondary amine of BPEI. It was reported that during thiolation reaction, the buffering capacity of BPEI was not changed significantly because primary and secondary amine groups are converted to higher order amine.[29] Therefore, endosomal escape ability of BPEI is retained after thiolation. After purification of BPEI-SH by precipitation in diethyl ether, sticky yellow product was obtained. Degree of thiolation was determined using ^{1}H NMR (Figure S2) and the conjugation ratio was calculated as 5.32 (Table 1). The disulfide crosslinked BPEI (BPEI-SS) was synthesized through the oxidization of BPEI-SH with DMSO. After purification by dialysis (MWCO = 10 kDa) against deionized water (DW) and lyophilization by freezing drying, we could acquire yellow solid, the BPEI-SS. The MW of BPEI1.2k and BPEI-SS was evaluated by gel permeation chromatography (GPC). By confirming that peaks of BPEI-SS appeared at earlier retention time compared to native BPEI1.2k, we could conclude that synthesized BPEI-SS has higher average MW than BPEI1.2k (Figure S3).

In order to introduce GE11 and bGE11 peptides to BPEI-SS, each type of GE11 peptides was firstly conjugated to the heterobifunctional polyethylene glycol (MAL-PEG-NHS). In each peptide, there is a free thiol in cysteine residue at the end of peptide sequence. This free thiol group can react with maleimide of MAL-PEG-NHS by Michael reaction. BPEI-SS-PEG-GE11 (or bGE11) was synthesized via the coupling reaction between NHS in resultant peptide-PEG-NHS and primary amine in BPEI-SS. After dialysis (MWCO = 10 kDa) against

DW and lyophilization, slightly yellow sponge-like powder was obtained. Successful conjugation between BPEI and PEG was confirmed by ^{1}H NMR (Figure S2). In ^{1}H NMR spectra, protons in BPEI and PEG main chains were found at δ 2.6-3.1 and δ 3.6. Using the relative integral values of the respective peaks in ^{1}H NMR, it was confirmed that molar ratio of PEG to BPEI was 0.16, 0.12 and 0.12 for BPEI-SS-PEG, BPEI-SS-PEG-GE11 and BPEI-SS-PEG-bGE11, respectively. The each conjugated peptide was quantified by measuring the fluorescence spectrometry. In the sequence of peptides, there are several aromatic amino acids such as tryptophan and tyrosine which can emit intrinsic fluorescence (excitation: 280 nm, emission: 350 nm).[30] Comparing the measured fluorescence intensity of GE11 or bGE11-tethered polymers with a calibration curve established by predetermined concentration of free peptide (Figure S4), the molar ratio of peptide to BPEI1.2k was estimated at 0.26 and 0.11 for BPEI-SS-PEG-GE11 and BPEI-SS-PEG-bGE11, respectively.

Physicochemical properties of polyplex

The cationic polymers can interact with negative charged plasmid DNA (pDNA) by electrostatic interaction. A resultant polyplex protects the gene from enzymes in blood flow as well as facilitates the cellular uptake of gene by condensing the pDNA with micro-size on a nano scale. Therefore, it is crucial for the successful gene delivery to demonstrate whether synthesized polymer can condense genes effectively. After preparation of each polyplexes at the various N/P ratios, condensing ability of polymers was evaluated by performing agarose gel retardation assay. BPEI25k was used as positive control. As shown in Figure 2A, while BPEI25k could retard pDNA completely at N/P > 1, BPEI-SS-PEG and BPEI-SS-PEG-GE11 (or bGE11) could retard pDNA completely at N/P > 10 and N/P > 5, respectively. Lower condensing ability of PEG-decorated polymers compared with BPEI25k could be attributed to the hindrance of the PEG chain to the interaction between BPEI and pDNA.[31] These results

indicate that BPEI-SS-PEG-GE11 (or bGE11) could successfully form the complex with pDNA.

The particle size and surface charge of polyplexes also affect the uptake and transfection *in vitro* and *in vivo*. To measure the size of the nanoparticles, polyplexes with various N/P ratios were analyzed by using dynamic light scattering (DLS). As shown in Figure 2B, the particle size of all polyplexes was decreased as the N/P ratios increased because of high electrostatic interaction by increased cationic charge. The size of BPEI-SS-PEG/pDNA and BPEI-SS-PEG-GE11/pDNA (or bGE11) was changed to around 200 nm at N/P ratio of 20 and 5, respectively, while these are above 2000 nm and 500 nm at N/P ratio of 1. These results indicate that all polymers at each proper N/P ratio could form the condensed nano-complex with pDNA.

Positively charged polyplexes have adhesion ability onto negatively charged plasma membrane of cells by electrostatic interaction. Therefore, it has been reported that positively charged polyplexes could internalize to the cell effectively.[32] As shown in Figure 2C, Zeta potential was increased as the increase of N/P ratio. In the case of BPEI-SS-PEG, polyplex showed negative zeta potential at N/P < 10, while it was positive at N/P ratio of 20. In addition, BPEI-SS-PEG-GE11/pDNA (or bGE11) at N/P ratio of 5 showed slightly positive zeta potential (± 5 mV).

In summary, the results of agarose gel retardation, DLS and zeta potential are correlated with each other and demonstrate that BPEI-SS-PEG-GE11 (or bGE11) polyplex have proper properties for *in vitro* and *in vivo* gene delivery.

Cytotoxicity

It is well-known that BPEI with high MW has toxicity to cells because positive charged

BPEI destabilizes the plasma membrane or interacts with cellular components especially, membrane of mitochondria.[33] To surmount these problems, disulfide linkage and PEG chains were introduced to the low MW of BPEI. The cytotoxicity of BPEI-SS-PEG-GE11 (or bGE11) polyplexes was evaluated by MTT assay in the EGFR-positive A549 and Huh-7 cells and the EGFR-negative NIH3T3 cell line (Figure 3). Naked pDNA and BPEI25k polyplexes at N/P ratio of 10 as a golden standard were used as control. The BPEI25k polyplex showed significant toxicity in all cell lines. However, there were no significant cytotoxicity in pDNA, BPEI-SS-PEG, BPEI-SS-PEG-GE11 (or bGE11), and BPEI-SS-PEG-bGE11 polyplexes regardless of EGFR receptor expression. These results could be attributed to the degradation ability of BPEI and outside exposure of PEG. BPEI-SS which is dissociated from polyplex may be degraded into low MW BPEI with low cytotoxicity in reductive condition of cytoplasm. In addition, BPEI and pDNA probably occupy the inner part of polyplex and PEG chain may be located outer part of polyplex. Therefore, the PEG could hamper the interaction between positively-charged BPEI and negatively-charged plasma membrane. These result confirmed the biocompatibility of the GE11- or bGE11-conjugated polymers.

In vitro transfection efficiency

In vitro gene transfection potential of the EGFR-targeted bioreducible polymers was investigated in EGFR-positive A549 and Huh-7 cell lines and EGFR-negative NIH3T3 cell line (Figure 4). Cells treated with naked pDNA and BPEI-SS-PEG polyplexes were used as controls. pDNA showed negligible transfection efficiency because it is difficult to be internalized into the cell. BPEI25K exhibited the most effective transfection efficiency with high cytotoxicity owing to the high density of positive charge (Figure 3 and Figure 4). As the N/P ratio increased, transfection efficiency of polymers increased in all cell lines. In EGFR-positive A549 and Huh-7 cell lines, GE11 or bGE11 tethered BPEI-SS polyplexes showed

enhanced transfection efficiency compared to non-targeted BPEI-SS-PEG polyplex at all N/P ratios. However, in EGFR-negative NIH3T3 cell line, non-targeted BPEI-SS-PEG polyplex showed much more transfection efficiency than GE11 or bGE11 tethered BPEI-SS polyplexes. These results demonstrated that GE11- or bGE11-conjugated gene carriers have a higher affinity to EGFR overexpressed cells than normal cells. Interestingly, BPEI-SS-PEG-bGE11 which has branched peptide could deliver pDNA effectively to the target cells compared to BPEI-SS-PEG-GE11. These results can be demonstrated by the hypothesis of EGFR dimerization.[34] It has been supposed that proper EGFR dimerization seems to be necessary for EGFR internalization. Applying this hypothesis, the branch structure of bGE11 having two adjacent ligands can form divalent interaction with EGFR, which facilitates the enhanced dimerization of the EGFR and receptor-mediated endocytosis compared to GE11. Although the dimerization of EGFR was not directly confirmed, it could be concluded that bGE11 tethered polyplex has a high transfection efficiency to EGFR overexpressed cancer cells.

Investigation of interaction between polyplex and plasma membrane

We hypothesized that bGE11 tethered polyplex has more chance to interact with EGFR, enhancing trafficking of the polyplex into the cell. In order to confirm the high interaction between bGE11 tethered polyplexes and EGFR, we carried out fluorescence-activated cell sorting analysis (FACS) (Figure 5). pDNA was labeled by YOYO-1 iodide before complexation with polymers. BPEI-SS-PEG, BPEI-SS-PEG-GE11 and BPEI-SS-PEG-bGE11 polyplexes at N/P ratio of 10 were transfected into EGFR-positive A549 and Huh-7 cell lines and EGFR-negative NIH3T3 cell line. Non-treated cells were used as controls. In EGFR-positive A549 and Huh-7 cell lines, GE11 and bGE11 tethered BPEI-SS polyplex showed enhanced interaction with plasma membrane compared to non-targeted polyplex due to the interaction between overexpressed EGFR and peptides. Especially, BPEI-SS-PEG-bGE11

polyplex showed higher interaction with EGFR-positive cells than BPEI-SS-PEG-GE11 polyplex. However, in EGFR-negative NIH3T3 cell line, non-targeted BPEI-SS-PEG polyplex demonstrated higher cellular uptake than BPEI-SS-PEG-GE11 (or bGE11) polyplexes. These results suggested that GE11 or bGE11 peptides enhance the cellular uptakes of polyplexes by receptor-mediated endocytosis and the higher affinity of bGE11 for EGFR facilitates the higher transfection efficiency compared to GE11 tethered polyplex.

***In vivo* fluorescence bio-imaging and *ex vivo* biodistribution**

Although targeting efficiency of GE11 and bGE11 peptide tethered BPEI-SS was successfully investigated *in vitro* level, these results cannot guarantee the effective clinical efficacy of developed polyplexes. Therefore, confirming the targeting ability of polyplexes *in vivo* is prerequisite for further clinical application. For *in vivo* fluorescence imaging, polymers were labeled with Cy5.5 before complexation with pDNA. We xenografted EGFR-positive A549 cells to female nude mice. *In vivo* experiment was performed when tumor had become appropriate size (~ 100 mm^3) for imaging. BPEI-SS-PEG, BPEI-SS-PEG-GE11 and BPEI-SS-PEG-bGE11 polyplexes were injected into the tail vein of each nude mouse. After 4 h from injection, *in vivo* fluorescence images were acquired (Figure 6A). Non-targeted BPEI-SS-PEG polyplex demonstrated low fluorescence signal (yellow) in tumor. However, BPEI-SS-PEG-GE11 and BPEI-SS-PEG-bGE11 polyplexes showed enhanced fluorescence signal at the tumor site compared to BPEI-SS-PEG/pDNA polyplex. Especially, BPEI-SS-PEG-bGE11 polyplex (red) showed the highest accumulation at the tumor site, which is consistent with *in vitro* transfection and FACS results.

In gene delivery system, it is expected that polyplexes should be mainly delivered into targeted tumor without non-specific delivery to the normal organs including spleen, lung, kidney, and etc. Therefore, biodistribution of polyplex was evaluated *ex vivo* level to confirm

the targeting ability (Figure 6B). After 24 h post-injection, all mice were sacrificed and fluorescence intensity of major organs was measured. In the case of BPEI-SS-PEG, fluorescence intensity of each organ was observed in the order of liver, lung, kidney, spleen and tumor. In the case of BPEI-SS-PEG-GE11, polyplex accumulation was confirmed in order of liver, kidney, spleen, lung and tumor. In BPEI-SS-PEG-bGE11 case, polyplexes were existed in order of liver, tumor, kidney, lung and spleen. As expected, BPEI-SS-PEG-bGE11/pDNA polyplex showed the highest accumulation of polyplex at tumor sites. These results clearly indicate that bGE11-conjugated polyplex can deliver gene to the targeted tumor effectively and reduce the non-specific delivery to the normal organs, showing the potential for use in treatments of EGFR overexpressed cancer.

Conclusions

In this study, we have developed an EGFR targeted bioreducible BPEI for efficient targeted gene delivery. EGFR targeted BPEI-SS showed efficient gene complexation ability, proper size and zeta potential for gene delivery *in vitro* and *in vivo*. Compared to non-targeted polymers, GE11- or bGE11-conjugated BPEI-SS showed enhanced transfection efficiency *in vitro* and tumor-targeted biodistribution *in vivo*. In addition, bGE11-conjugated polymers showed higher targeting ability than GE11-conjugated polymers due to multivalent interaction between ligand and receptor. Taken together, our results suggest that branched structure of targeting ligand will be one of strategy to design efficient targeted delivery system.

Acknowledgements

This work was supported by the Research Center Program of IBS (Institute for Basic Science) in Korea (CA1203-02) and Converging Research Center Program (2012K001474) through an NRF grant funded by the Korean government (MEST).

Electronic Supplementary Information (ESI) available: Synthetic scheme and figures of ^{1}H NMR, GPC of delivery carriers and calibration curve of each peptide. See DOI: 10.1039/b000000x/

Notes and references

1. S. D. Li and L. Huang, *Gene Ther.*, 2006, **13**, 1313.

2. J. Sudimack and R. J. Lee, *Adv. Drug Deliv. Rev.*, 2000, **41**, 147.

3. F. Danhier, O. Feron and V. Préat, *J. Control. Release*, 2010, **148**, 135.

4. A. C. Antony, *Ann. Rev. Nutr.*, 1996, **16**, 501.

5. E. Ruoslahti and M. D. Pierschbacher, *Science*, 1987, **238**, 491.

6. R. Pasqualini, E. Koivunen, R. Kain, J. Lahdenranta, M. Sakamoto, A. Stryhn, R. A. Ashmun, L. H. Shapiro, W. Arap and E. Ruoslahti, *Cancer Res.*, 2000, **60**, 722.

7. J. Mendelsohn and J. Baselga, *Oncogene*, 2000, **19**, 6550.

8. C. Yewale, D. Baradia, I. Vhora, S. Patil and A. Misra, *Biomaterials*, 2013, **34**, 8690.

9. R. S. Herbst, *Int. J. Radiat. Oncol.*, 2004, **59**, S21.

10. A. A. Bhirde, V. Patel, J. Gavard, G. Zhang, A. A. Sousa, A. Masedunskas, R. D. Leapman, R. Weigert, J. S. Gutkind and J. F. Rusling, *ACS Nano*, 2009, **3**, 307.

11. E. Bohl Kullberg, N. Bergstrand, J. Carlsson, K. Edwards, M. Johnsson, S. Sjöberg and L. Gedda, *Bioconjug. Chem.*, 2002, **13**, 737.

12. J. Capala, R. F. Barth, M. Bendayan, M. Lauzon, D. M. Adams, A. H. Soloway, R. A. Fenstermaker and J. Carlsson, *Bioconjug. Chem.*, 1996, **7**, 7.

13. H. Lee, T. H. Kim and T. G. Park, *J. Control. Release*, 2002, **83**, 109.

14. K. Oda, Y. Matsuoka, A. Funahashi and H. Kitano, *Mol. Syst. Biol.*, 2005, **1**, 2005.0010.

15. Z. Li, R. Zhao, X. Wu, Y. Sun, M. Yao, J. Li, Y. Xu and J. Gu, *FASEB J.*, 2005, **19**, 1978.

16. Y. Guo, H. Feinberg, E. Conroy, D. A. Mitchell, R. Alvarez, O. Blixt, M. E. Taylor, W. I. Weis and K. Drickamer, *Nat. Struct. Mol. Biol.*, 2004, **11**, 591.

17. R. C. Ladner, *Trends Biotechnol.*, 1995, **13**, 426.

18. Á. Roxin and G. Zheng, *Future Med. Chem.*, 2012, **4**, 1601.

19. G. Colombo, F. Curnis, G. M. S. De Mori, A. Gasparri, C. Longoni, A. Sacchi, R. Longhi and A. Corti, *J. Biol. Chem.*, 2002, **277**, 47891.

19. E. Koivunen, B. Wang and E. Ruoslahti, *Nat Biotech*, 1995, **13**, 265.

20. S. Verrier, S. Pallu, R. Bareille, A. Jonczyk, J. Meyer, M. Dard and J. Amédée, *Biomaterials*, 2002, **23**, 585.

21. M. Mammen, S.-K. Choi and G. M. Whitesides, *Angew. Chem. Int. Ed.*, 1998, **37**, 2754.

22. W. J. Lees, A. Spaltenstein, J. E. Kingery-Wood and G. M. Whitesides, *J. Med. Chem.*, 1994, **37**, 3419.

23. H. Chen and M. L. Privalsky, *Proc. Natl. Acad. Sci. USA*, 1995, **92**, 422.

24. J. M. Davie and W. E. Paul, J. Exp. Med., 1972, **135**, 643.

25. S. Son, K. Singha and W. J. Kim, *Biomaterials*, 2010, **31**, 6344.

26. S. Son, D. W. Hwang, K. Singha, J. H. Jeong, T. G. Park, D. S. Lee and W. J. Kim, *J. Control. Release*, 2011, **155**, 18.

27. D. W. Hwang, S. Son, J. Jang, H. Youn, S. Lee, D. Lee, Y.-S. Lee, J. M. Jeong, W. J. Kim

and D. S. Lee, *Biomaterials*, 2011, **32**, 4968.

28. D. Fischer, T. Bieber, Y. Li, H.-P. Elsässer and T. Kissel, *Pharm. Res.*, 1999, **16**, 1273.

29. Q. Peng, Z. Zhong and R. Zhuo, *Bioconjug. Chem.*, 2008, **19**, 499.

30. F. W. J. Teale and G. Weber, *Biochem. J.*, 1957, **65**, 476.

31. J. H. Choi, J. S. Choi, H. Suh and J. S. Park, *Bull. Korean. Chem. Soc.*, 2001, **22**, 46.

32. Z. -G. Yue, W. Wei, P. -P. Lv, H. Yue, L. -Y. Wang, Z. -G. Su and G. -H. Ma, Biomacromolecules, 2011, **12**, 2440.

33. S. M. Moghimi, P. Symonds, J. C. Murray, A. C. Hunter, G. Debska and A. Szewczyk, *Mol. Ther.*, 2005, **11**, 990.

34. Q. Wang, G. Villeneuve and Z. Wang, *EMBO Rep.*, 2005, **6**, 942.

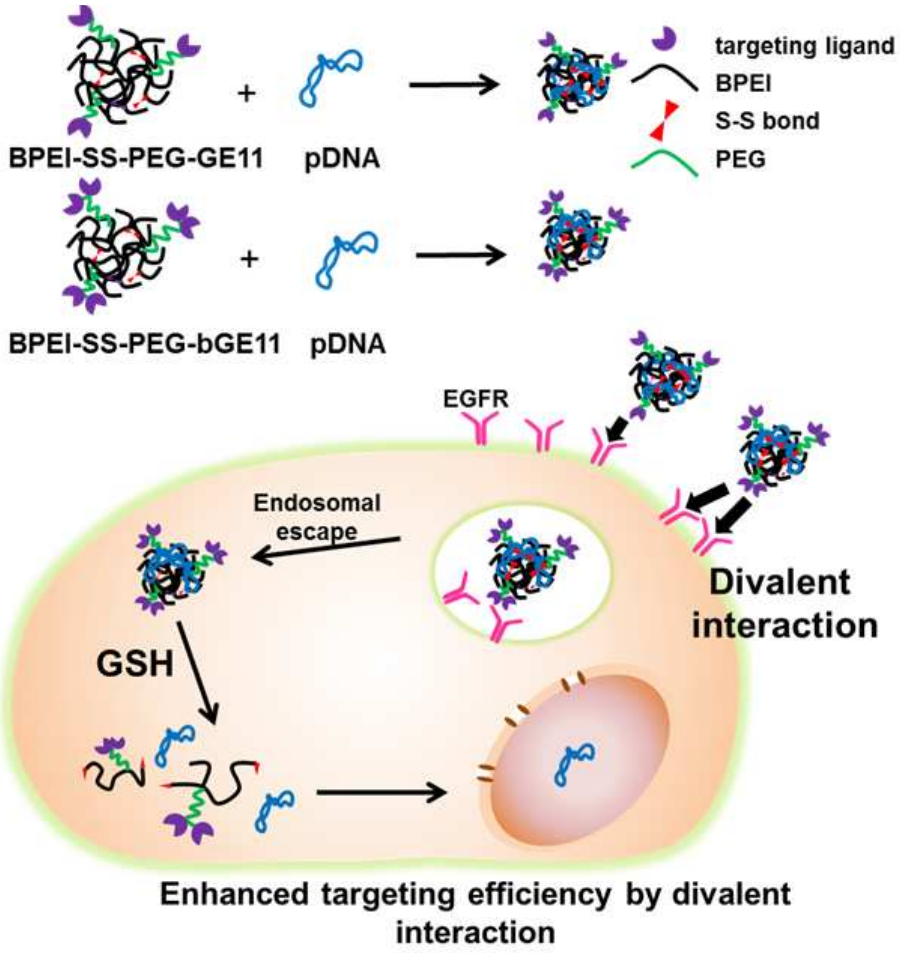

Figure 1. Schematic diagram of gene delivery by using EGFR targeted bioreducible polyethylenimine.

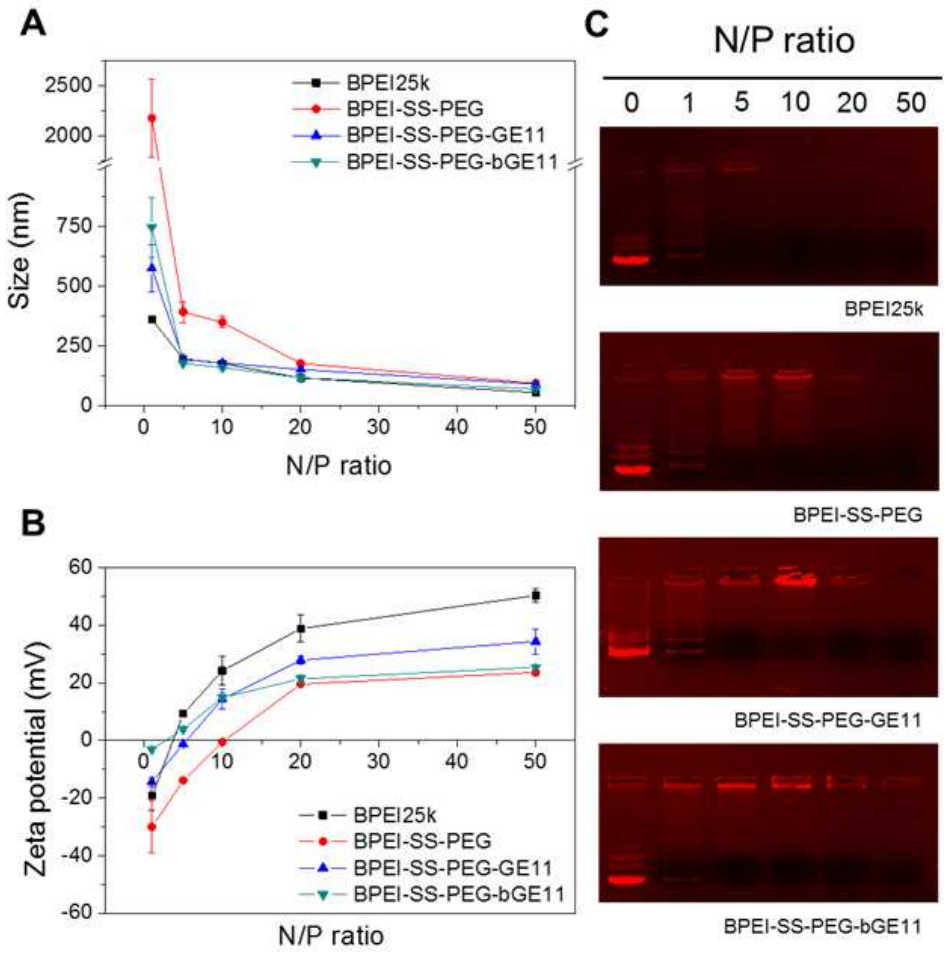

Figure 2. Physicochemical property of polyplex. (A) Agarose gel retardation assay, (B) size and (C) zeta potential of polyplexes of BPEI25k, BPEI-SS-PEG, BPEI-SS-PEG-GE11, and BPEI-SS-PEG-bGE11 at various N/P ratios. Data represent mean ± SD (n=3).

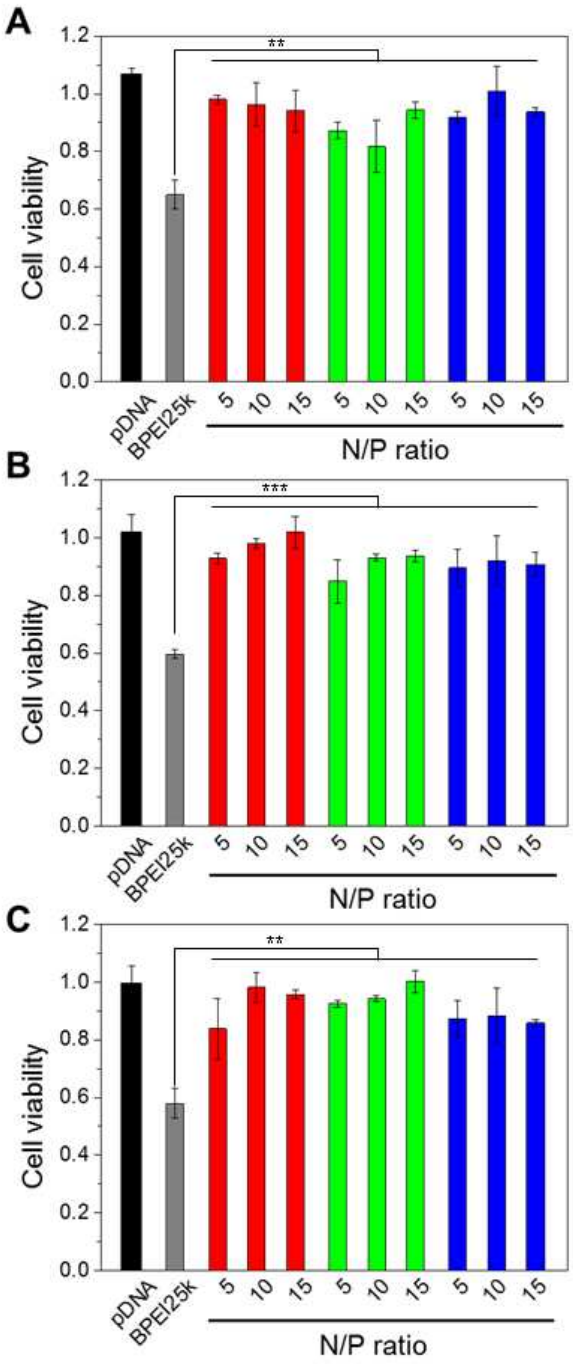

Figure 3. Cell viability. EGFR-positive (A) A549 and (B) Huh-7 cell lines and EGFR-negative (C) NIH3T3 cell line were treated with pDNA (black), BPEI25k (gray) at N/P ratio 10, and BPEI-SS-PEG (red), BPEI-SS-PEG-GE11 (green) and BPEI-SS-PEG-bGE11 (blue) at various N/P ratios. Data represent mean ± SD (n=5; ***P<0.01*).

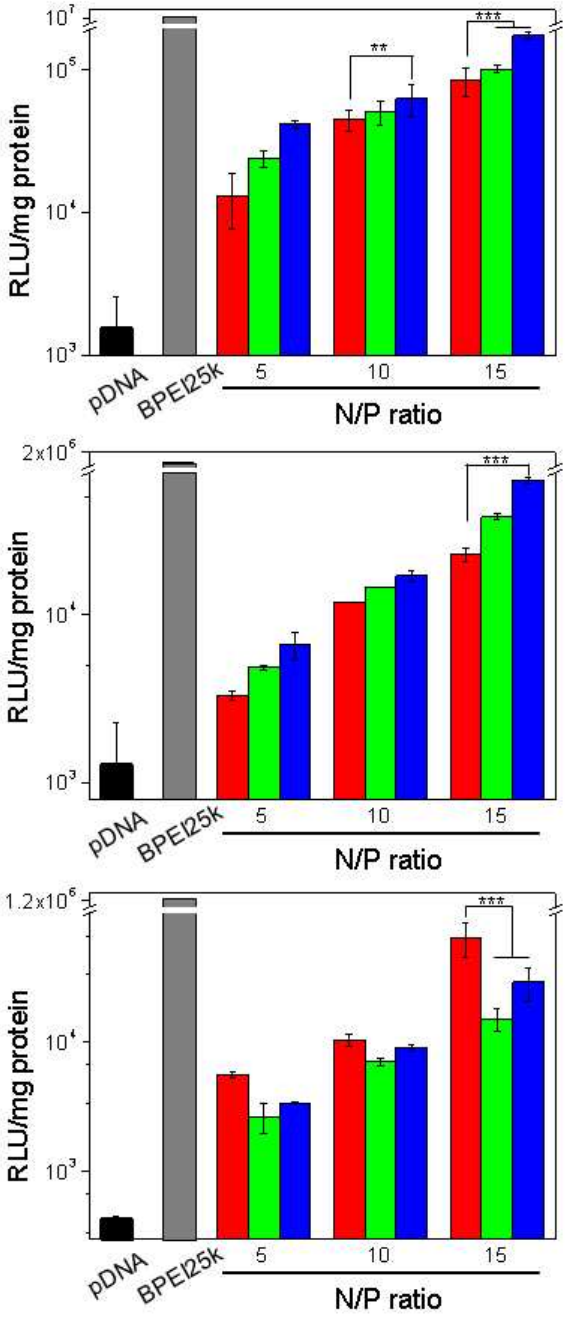

Figure 4. *In vitro* transfection efficiency. EGFR-positive (A) A549 and (B) Huh-7 cell lines and EGFR-negative (C) NIH3T3 cell line were treated with pDNA (black), BPEI25K (gray) BPEI-SS-PEG (red), BPEI-SS-PEG-GE11 (green) and BPEI-SS-PEG-bGE11 (blue) at N/P ratio 5, 10, and 15. Data represent mean ± SD (n=3; ***P<0.01, ***P<0.001*).

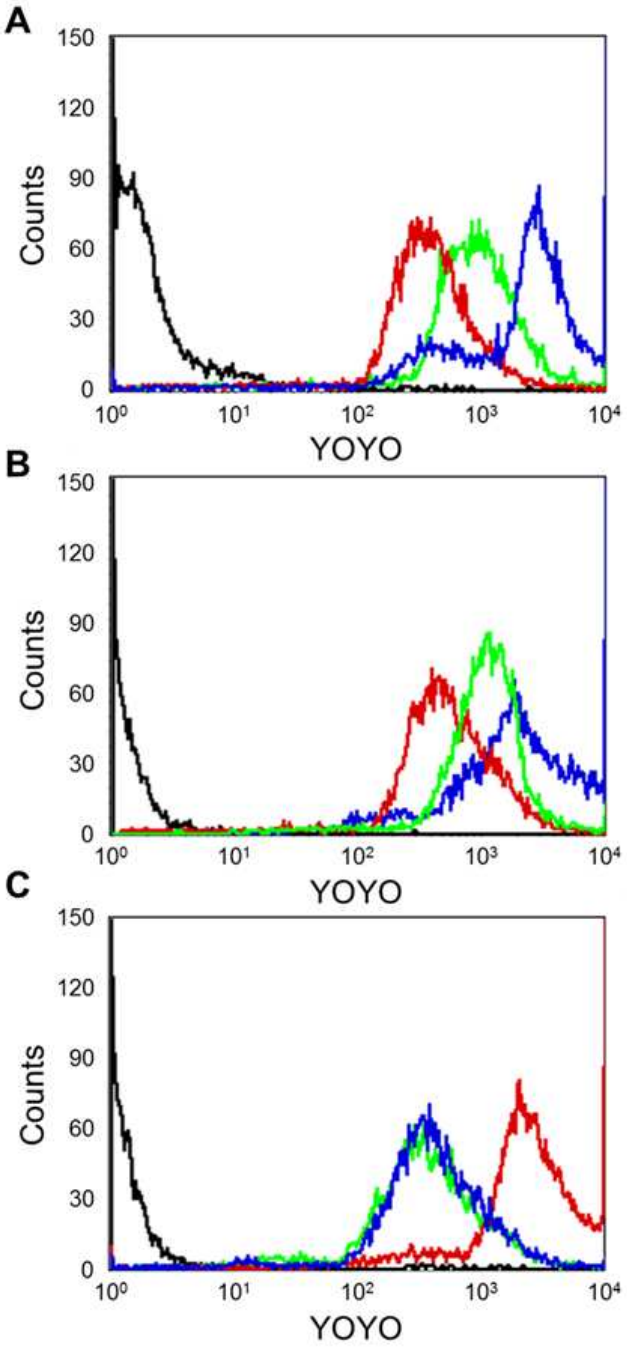

Figure 5. FACS histogram. Analysis of EGFR-positive (A) A549 and (B) Huh-7 cell lines and EGFR-negative (C) NIH3T3 cell line treated with YOYO-labeled polyplexes of BPEI-SS-PEG (red), BPEI-SS-PEG-GE11 (green) and BPEI-SS-PEG-bGE11 (blue) at N/P ratio of 10. 1×10^4 cells were counted in each sample by FACS.

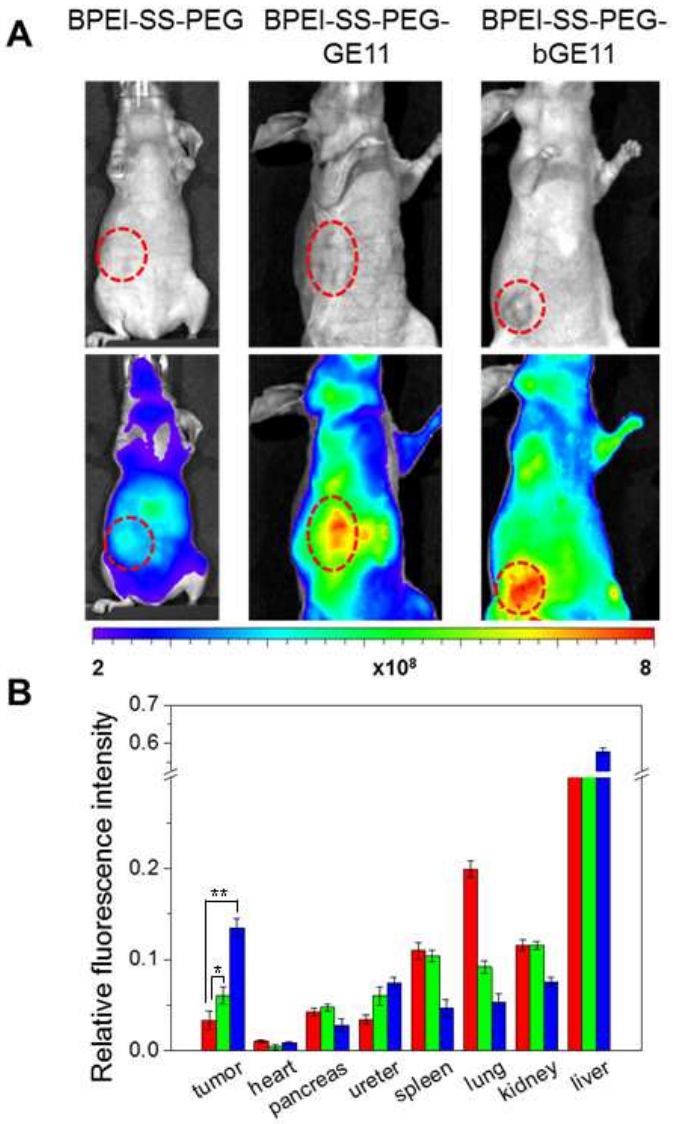

Figure 6. *In vivo* imaging and biodisribution of polyplexes in tissue and major organs. (A) *In vivo* imaging of A549 xenografted mice. Images were taken after 4 h from intravenously injection of Cy5.5 labeled polyplexes. (B) Quantitative analysis of relative organ accumulation retrieved from tumor bearing mice after 24 h from injection of BPEI-SS-PEG (red), BPEI-SS-PEG-GE11 (green) and BPEI-SS-PEG-bGE11 (blue) polyplexes. Data represent mean ± SE (n=3; *$P<0.05$, **$P<0.01$).

Table 1. Characterization of BPEI-SS-PEG and BPEI-SS-PEG-peptide polymers

Denotation	Thiol[a]	PEG[b]	peptide[c]
BPEI-SS-PEG		0.16	-
BPEI-SS-PEG-GE11	5.32	0.12	0.26
BPEI-SS-PEG-bGE11		0.12	0.11

[a] measured by ^{1}H NMR. molar ratio of thiol group/BPEI1.2k chain in polymers, [b] confirmed by ^{1}H NMR. molar ratio of PEG to BPEI1.2k, [c] confirmed by fluorescence spectrometry. molar ratio of GE11 or bGE11 peptide to BPEI1.2k.